

A flammability performance comparison between synthetic and natural clays in polystyrene nanocomposites

Alexander B. Morgan^{1,*;†}, Lih-Long Chu² and Joseph D. Harris³

¹*Inorganic Materials Group, Corporate R&D, The Dow Chemical Company, U.S.A.*

²*Engineering Compounds Group, Engineering Plastics Business, The Dow Chemical Company, U.S.A.*

³*Analytical Sciences, Corporate R&D, The Dow Chemical Company, U.S.A.*

SUMMARY

Polymer-clay nanocomposites are a newer class of flame retardant materials of interest due to their balance of mechanical, thermal and flammability properties. Much more work has been done with natural clays than with synthetic clays for nanocomposite flammability applications. There are advantages and disadvantages to both natural and synthetic clay use in a nanocomposite, and some of these, both fundamental and practical, will be discussed in this paper.

To compare natural and synthetic clays in regards to polymer flammability, two clays were used. The natural clay was a US mined and refined montmorillonite, while the synthetic clay was a fluorinated synthetic mica. These two clays were used as inorganic clays for control experiments in polystyrene, and then converted into an organoclay by ion exchange with an alkyl ammonium salt. The organoclays were used to synthesize polystyrene nanocomposites by melt compounding. Each of the formulations was analysed by X-ray diffraction (XRD), thermogravimetric analysis (TGA) and transmission electron microscopy (TEM). Flammability performance was measured by cone calorimeter.

The data from the experiments show that the synthetic clay does slightly better at reducing the heat release rate (HRR) than the natural clay. However, all the samples, including the inorganic clay polystyrene microcomposites, showed a decreased time to ignition, with the actual nanocomposites showing the most marked decrease. The reason for this is postulated to be related to the thermal instability of the organoclay (via the quaternary alkyl ammonium). An additional experiment using a more thermally stable organoclay showed a time to ignition identical to that of the base polymer.

Finally, it was shown that while polymer-clay nanocomposites (either synthetic or natural clay based) greatly reduce the HRR of a material, making it more fire safe, they do not provide ignition resistance by themselves, at least, at practical loadings. Specifically, the cone calorimeter HRR curve data appear to support that these nanocomposites continue to burn once ignited, rather than self-extinguish. Copyright © 2004 John Wiley & Sons, Ltd.

KEY WORDS: polymer-clay nanocomposites; synthetic clay; montmorillonite; flame retardant

*Correspondence to: Alexander B. Morgan, The Dow Chemical Company, 1776 Building Door A, Midland, MI, 48674, USA.

† E-mail: abmorgan@dow.com

1. INTRODUCTION

Polymer-clay nanocomposites have generated a great deal of interest due to the improvements in mechanical [1] and flammability properties [2–6]. They are one of the few classes of flame retarded materials in which the flame retardant imparts an improvement in both mechanical and flammability properties [7]. A flame retardant usually provides an improvement in flammability at the expense of mechanical properties. Since polymer-clay nanocomposites provide a balance of these properties, they are attractive for commercial flame retarded products.

The key component of the polymer-clay nanocomposite is the organoclay, which is prepared from inorganic clay. The choice of inorganic clay is important, because not all clays can be used for nanocomposite synthesis. The clay used must be dispersible in water, and capable of ion exchange with ionic surfactants. In addition to this limitation, it must be stressed that no two clays are alike, as each has its own unique structure, aspect ratio and chemistry. This issue is further complicated with the use of natural and synthetic clays.

Natural clays are mined and refined prior to use. However, the refining process adds cost to the clay and the ion exchange to the final organoclay. There is another issue that comes from the natural processes of clay formation. Even when two clays are classified to be of the same class, they are only identical if mined from the same location and mineral vein, and even in such cases there can be some differences. For example, montmorillonite clay from the southern United States of America is not the same as montmorillonite clay from Montmorillonais, France. Montmorillonite mined from Cheto, Arizona, USA is different to montmorillonite from Otay, California, USA, which is different to the clay from Itoigawa, Niigata, Japan [8]. The trace metals, aspect ratios and cation exchange capacity of these clays may be very different. One recent paper has shown the iron content in montmorillonite can affect polymer nanocomposite flammability, so the issue of trace metal content could be important [9]. Due to these differences, if the same type of natural clay is used, an industrial producer may not be able to make the same product at various locations around the globe. Local sources of clays could give different results for the same formulation, thus requiring fine tuning of the formulation for each site where the product is produced. Further, many natural clays impart color (usually brown to yellow) to the final polymer formulation; therefore it is difficult to make a colorless nanocomposite out of natural clay. This can be a limitation in some applications for the final product.

Synthetic clays are also layered silicates, but there is more control in the chemical structure, aspect ratio, cation exchange capacity and trace elements. Provided the production conditions are kept the same, each batch of synthetic clay is the same as the last, and therefore, some of the structural and compositional issues with natural clays can be avoided, or reduced, with a synthetic clay. However, inorganic synthetic clays tend to be more expensive than mined and refined natural clays. The main advantage with the synthetic clay is that its consistency allows possible production of a global product with consistent results. Also, most, but not all, synthetic clays are white, and do not impart color to the final nanocomposite. When the appearance of a final product is essential, a white background is preferred to yellow or brown. When considering the issues presented above, the present study compares a natural clay and synthetic clay side by side to determine how the different clays affected the flammability of a polystyrene nanocomposite.

With the choice of clay considered, the organic treatment to be used on the organoclay must be considered as well. Polymer-clay nanocomposites can be synthesized in a number of ways [1], but an organic treatment is needed to ensure compatibility between the normally hydrophobic

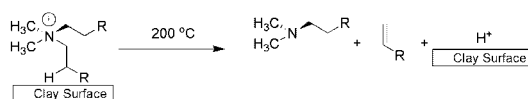


Figure 1. Hoffman degradation of an alkyl ammonium organic treatment.

polymer and a hydrophilic clay. The organic treatment typically converts the surface of the hydrophilic inorganic clay to a hydrophobic surface, allowing the polymer and modified clay surface to interact and form a nanocomposite. The most commonly used organic treatment to make organoclays today is ion exchange with alkyl ammonium salts. These treatments are commercially available for a variety of applications, but many of them have readily found use in organoclay synthesis. With regard to flame retardancy, the organic treatment's reaction to fire and the residual clay structure formed are important in the understanding of polymer nanocomposite flammability.

Alkyl ammonium organic treatments are thermally unstable above 200°C [10–12]. Therefore, under fire conditions, heat may decompose not just the polymer but also the organic treatment at the interface between the polymer and clay. The decomposition of the alkyl ammonium occurs via the Hoffman elimination reaction (Figure 1). In the Hoffman degradation, the beta hydrogen on the alkyl group is eliminated, giving an alpha olefin and a free amine. The proton from the beta-elimination reaction then goes to the clay surface, whereupon it forms the acidic clay site. Once the organic treatment is decomposed, the acidic site has direct interface with the remaining polymer. Layered silicates (clays) in the acid form are known to cause hydrocarbon cracking and/or hydrocarbon aromatization, depending on silicate structure and acidity [13]. It is possible that the acid site formed is responsible for the char formation observed with polymer nanocomposites under fire conditions [14,15].

The issue of organic treatment degradation is a very important issue as the decomposition can cause a quick release of fuel early in the ignition process and make the nanocomposite easier to ignite than the base polymer. This has been seen with cone calorimeter data in numerous studies [2–5,16,17]. Further, there is the need to melt-compound the clay and polymer to form the nanocomposite; having the materials degrade at or below processing conditions presents a problem. If the organic treatment decomposes during melt-compounding, then the polymer will de-intercalate from the plastic during processing, resulting in a microcomposite rather than a nanocomposite [2,18].

In this study, two clays were compared: a natural clay, montmorillonite (MMT), and a synthetic clay, fluorinated synthetic mica (FSM). With these two clays both the inorganic clay (sodium exchanged) and the organoclay were used. The inorganic clay, once compounded into PS, became a microcomposite, but it served as a control sample to compare with other published results on PS nanocomposites [16]. The organic treatment was a dimethyl, bis(hydrogenated tallow) ammonium treatment, for both the FSM and MMT clays. An additional experiment with a more thermally stable phosphonium organic treatment, *n*-hexadecyl triphenylphosphonium, was done with the FSM clay to see how improved thermal stability of the organic treatment affected polymer flammability with regard to the Hoffman degradation mentioned above. While the use of the organo MMT in PS has been reported in the open literature [2,16], cone calorimeter data for the organo FSM has not been reported to the best of our knowledge. Finally, the effects of clay loading on the flammability of the resulting PS nanocomposites were investigated. Three different loadings for each clay were studied, a low level (1 wt% inorganic), a

medium level (5 wt% inorganic) and a high level (10 wt% inorganic). The term 'inorganic' here is used to refer to the total amount of inorganic clay in the final formulation, not the total amount of clay. For example, if an organoclay is used, due to the organic treatment, 10 wt% inorganic content would be 18.6 wt% O-FSM. This point becomes more clear in the experimental section and Table I below.

2. EXPERIMENTAL

2.1. Materials

The clays used in this study were obtained from various sources. Sodium fluorinated synthetic mica (NaFSM) was obtained from Co-op Chemical of Japan, under the trade name of Somasif ME-100. Organo FSM [dimethyl, di(hydrogenated tallow) ammonium treated FSM, or O-FSM] and Triphenyl, *n*-hexadecyl phosphonium treated FSM [P-FSM] were synthesized internally at Dow using typical organoclay synthesis procedures. Sodium montmorillonite (NaMMT) was obtained from Southern Clay Products, under the trade name of Cloisite Na⁺. Organo montmorillonite [dimethyl, di(hydrogenated tallow) ammonium treated MMT or O-MMT] was obtained from Southern Clay Products, under the trade name of Cloisite 15A. Polystyrene (Styron 612) and polystyrene-co-maleic anhydride were obtained from the Dow Chemical Company.

2.2. Formulations/processing

All samples were compounded with a Haake Rheocord melt compounder with a 250 cc mixing head. The melting temperatures were set at 200°C with a mixing speed for the rollers set to 60 rpm. The components of each sample were dry blended in a plastic bag and then fed into the mixing bowl gradually until the maximum torque was observed. Mixing was continued for 3 more minutes after maximum torque. Polymer samples were then molded via compression molding to produce cone calorimeter plaques (4" × 4" × 1/8" or 101.6 mm × 101.6 mm × 3.175 mm) for testing. The mold temperature was set at 200°C and the heating, holding and cooling times were 10, 2 and 10 min, respectively.

2.3. Analysis techniques

Thermogravimetric analysis (TGA) data were collected with a TA Instruments TGA 2950, under nitrogen, at 20°C/min, from 25°C to 700°C. X-ray diffraction data (XRD) were collected on a Bruker AXS diffractometer using Cu K α radiation ($\lambda = 0.1505945$ nm) with a 0.02 2θ step size and a 2 s count time. Samples used for XRD were ground to a particle size of <40 μ m or were analysed as a solid monolith (25 mm × 25 mm × 3 mm thick),[‡] and were placed in a horizontal configuration (transmission) for collection of XRD data. All samples were analysed while in synchronous rotation mode, to eliminate as many as possible orientation effects. Nanocomposites were viewed by transmission electron microscopy by having the nanocomposite thin-sectioned using a Reichert-Jung Cryo-Ultracut E (Serial 393365) at 25°C and collected on a copper grid. Sections were examined with a Philips CM-12 TEM (Serial D769) running at

[‡]PS samples can be put (carefully) with a hobby hack saw to give samples of the proper size.

Table I. PS + clay formulations.

Sample ID	PS+ 1 wt% NaFSM		PS+ 5 wt% NaFSM		PS+ 10 wt% NaFSM		PS+ 1 wt% O-FSM		PS+ 5 wt% O-FSM		PS+ 10 wt% O-FSM		PS+ 1 wt% NaMMT		PS+ 5 wt% NaMMT		PS+ 10 wt% NaMMT		PS+ 1 wt% O-MMT		PS+ 5 wt% O-MMT		PS+ 10 wt% O-MMT		PS+ SMA Control		PS+ SMA P-FSM			
	NaFSM	PS	NaFSM	PS	NaFSM	PS	NaFSM	PS	NaFSM	PS	NaFSM	PS	NaFSM	PS	NaFSM	PS	NaFSM	PS	NaFSM	PS	NaFSM	PS	NaFSM	PS	NaFSM	PS	NaFSM	PS	NaFSM	
PS	99	0	95	0	90	0	96.1	0	90.7	0	81.4	0	99	0	95	0	90	0	98.4	0	91.9	0	83.8	0	90	0	91.7	0	82.5	0
NaFSM	1	5	0	0	10	0	0	0	0	0	0	0	0	0	0	0	0	0	0	0	0	0	0	0	0	0	0	0	0	0
O-FSM	0	0	0	1.9	0	18.60	0	9.3	0	0	0	0	0	0	0	0	0	0	0	0	0	0	0	0	0	0	0	0	0	0
NaMMT	0	0	0	0	0	0	0	0	0	1	0	0	1	5	10	0	0	0	0	0	0	0	0	0	0	0	0	0	0	0
O-MMT	0	0	0	0	0	0	0	0	0	0	0	0	0	0	0	0	0	0	1.6	8.10	16.2	0	0	0	0	0	0	0	0	0
SMA	0	0	0	0	0	0	0	0	0	0	0	0	0	0	0	0	0	0	0	0	0	0	0	0	10	0	0	0	9.2	
P-FSM	0	0	0	0	0	0	0	0	0	0	0	0	0	0	0	0	0	0	0	0	0	0	0	0	0	0	8.3	0	8.3	

an accelerating voltage of 120 kV. Images were recorded digitally with a Gatan Multiscan CCD camera, Model 749 (Serial 971119010). Cone calorimeter experiments were analysed on a Dark Star Research Cone Calorimeter at 35 kW/m² heat flux and exhaust flow of 241/s using the standardized cone calorimeter procedure (ASTM E-1354-99). Data collected are the average of three samples, with an error of $\pm 10\%$.

3. RESULTS AND DISCUSSION

A total of 16 samples (Table I) were analysed by cone calorimeter to compare the possible effects of clay type (natural vs synthetic) on polymer flammability. Pictures were taken of the material after testing to show the presence or absence of char from the nanocomposite or microcomposite, respectively.

T_{ig} time to ignition; peak q, peak heat release rate (HRR);
 mean q, average HRR; 180sec q, HRR at 180s into test;
 300sec q, HRR at 300s into test; total q, total HRR;
 effective H, effective heat output energy per kg
 of material.

Along with the HRR curves, the mass-loss rate (MLR) data are shown. MLR data, combined with HRR data, can sometimes give insights into a condensed phase or vapor phase mechanism of flame retardancy. Along with the cone calorimeter, each sample was analysed by XRD, TEM and TGA. This was done to help relate the effects of the flammability reduction to clay loadings and clay dispersion.

3.1. Cone calorimeter results

The data in Table II show the overall data for the six FSM samples analysed in this study. NaFSM is the non-treated (inorganic) form of this clay, and it will only form microcomposites due to a lack of organic treatment. When compared with the PS control, all the samples show reduced HRR values. However, the microcomposite samples (NaFSM samples) show very little

Table II. Cone calorimeter summary for PS + FSM samples.

Product	Units	PS+ 1 wt% NaFSM	PS+ 5 wt% NaFSM	PS+ 10 wt% NaFSM	PS+ 1.9 wt% O-FSM	PS+ 9.3 wt% O-FSM	PS+ 18.6 wt% O-FSM	PS control
T_{ig}	s	52	43	41	63	49	51	65
Peak q	kW/m ²	1201.3	1146.2	995.1	910.6	428.4	513.3	1293.6
Mean q	kW/m ²	756.9	722.8	612.9	585.3	325.3	269.6	692.4
180sec q	m ² /kg	651.8	652.5	626.7	613.1	392.0	356.8	614.1
300sec q	kW/m ²	391.1	391.5	376.2	368.6	325.3	303.8	368.4
Total q	MJ/m ²	117.2	117.4	112.8	110.6	97.6	93.6	110.5
Effective H	MJ/kg	31.9	31.7	30.8	29.4	27.1	27.9	30.6

reduction in HRR which is similar to data seen elsewhere with sodium clays in PS [16]. The HRR reduction for these microcomposites is due to fuel load reduction, which was accomplished with the use of inorganic filler. It is surprising that the NaFSM samples all show earlier T_{ig} than the PS control. This could be due to the presence of catalytic sites in the clay.

For the O-FSM nanocomposites, the reduction in FSM is dramatic, with peak HRR reductions of 60% to 67%. Interestingly, the 18.6 wt% O-FSM sample has a higher peak HRR than the 9.3 wt% O-FSM sample, but a lower average HRR value. This difference is believed to be caused by the higher loading of organic treatment in this sample. While the nanocomposites show reduced HRR values, the T_{ig} times are shortened. The T_{ig} becomes shorter with increasing amounts of inorganic content across all samples, with the exception of the 9.3 and 18.6 wt% O-FSM samples, where the T_{ig} are about the same. The HRR curves shown in Figure 2 fit nicely with the mass loss rate curves in Figure 3. This suggests, as was previously indicated in the literature [2,3], that the mechanism of flame retardancy occurs in the condensed phase. The clay slows down the rate of fuel (mass) loss, and therefore lowers the average HRR while increasing burn times. Along with the impressive HRR reductions is the formation of char seen with the O-FSM samples, Figures 4 and 5 show the residue of the NaFSM microcomposite and O-FSM nanocomposite after burning. The NaFSM microcomposite (Figure 4) only shows some soot and the white FSM residue. The O-FSM sample (Figure 5) shows a thick black char.

The MMT samples (Table III) show a similar trend to the FSM samples (Table II). As was seen with the other microcomposites, the NaMMT microcomposites did not greatly reduce the HRR of the sample, but did lower T_{ig} . Again, the lowering of T_{ig} was a surprising result as it was thought that the clay would have minimal influence on the polymer as a whole. The O-MMT samples showed reduced HRR values, though not quite as much as the FSM samples. As with the O-FSM samples, the low weight loading nanocomposite sample does not appear different from the microcomposite samples when looking at the HRR curves (Figure 6). Another difference between the O-MMT nanocomposites and the other samples is the T_{ig} . The T_{ig} for the O-MMT samples are not as severely reduced as they are for the O-FSM samples. The

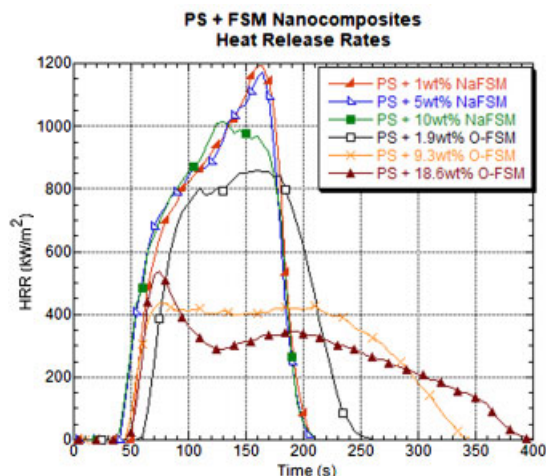


Figure 2. HRR curves for polystyrene (PS) + fluorinated synthetic mica (FSM) samples.

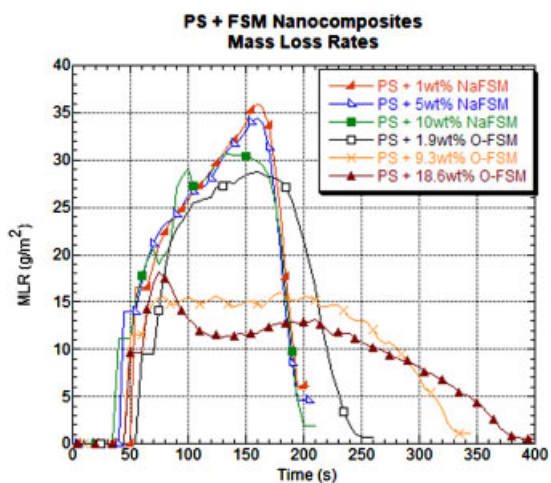


Figure 3. Mass loss rate (MLR) curves for PS + fluorinated synthetic mica (FSM) samples.



Figure 4. [Left] PS + 10 wt% NaFSM sample after burning.



Figure 5. [Right] PS + 18.6 wt% O-FSM sample after burning.

Table III. Cone calorimeter results for polystyrene (PS) + Montmorillonite (MMT) samples.

Product	Units	PS+1 wt%	PS+5 wt%	PS+10 wt%	PS+1.9 wt%	PS+9.3 wt%	PS+18.6 wt%	PS control
		NaMMT	NaMMT	NaMMT		O-MMT	O-MMT	
T_{ig}	s	57	41	40	66	58	52	65
Peak q	kW/m ²	110.75	993.1	791.9	1079.5	554.9	445.8	1293.6
Mean q	kW/m ²	688.4	630.7	591.2	674.8	365.8	267.2	692.4
180sec q	m ² /kg	611.1	616.0	591.2	618.0	459.3	345.5	614.1
300sec q	kW/m ²	366.7	369.9	354.7	370.8	326.2	306.8	368.4
Total q	MJ/m ²	110.0	110.9	106.4	111.2	97.8	96.7	110.5
Effective H	MJ/kg	29.8	29.5	29.2	29.9	26.6	26.9	30.6

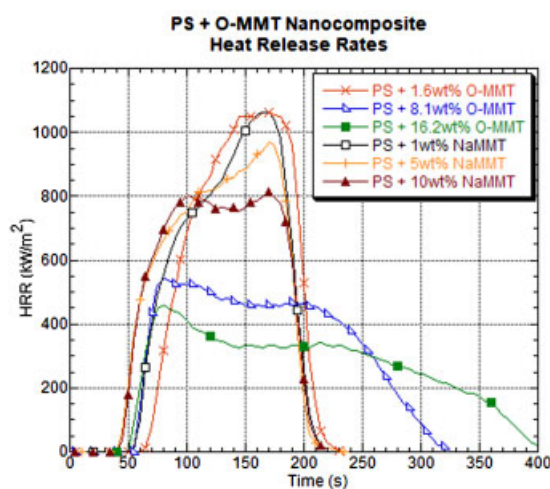


Figure 6. HRR curves for polystyrene (PS) + Montmorillonite (MMT) samples.

O-MMT does have less organic treatment when compared with the O-FSM; therefore, the T_{ig} reductions could be related to organic treatment concentration. The MLR data (Figure 7) are similar to the other samples in that they match closely the HRR data (Figure 6). This suggests again that clay decreases the rate of fuel release during burning.

The char obtained by the MMT materials, however, is a bit different when compared with the char from the FSM samples. Specifically, the NaMMT sample is dark gray (Figure 8), suggesting that more carbon is trapped in the char residue. The char remaining from the O-MMT nanocomposite (Figure 9) is black and thick, as was the char from the O-FSM sample (Figure 5), suggesting the presence of carbonaceous char.

The data for the PS + Phosphonium treated FSM (P-FSM) samples were only collected on 8.3 wt% P-FSM samples. The only difference between the two nanocomposite samples was that a compatibilizer (polystyrene-co-maleic anhydride, or SMA) was used in one sample. As can be seen from the data in Table IV, the nanocomposites show dramatically reduced HRR values. The major improvement in these samples when compared with the O-MMT or the O-FSM samples is that the P-FSM does not seem to cause reduced T_{ig} . Since TGA data have shown the

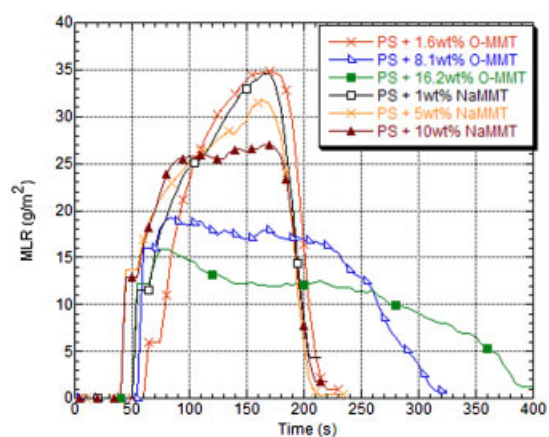


Figure 7. Mass loss rate (MLR) curves for PS + Montmorillonite (MMT) samples.



Figure 8. [Left] PS + 10 wt% NaMMT sample after burning.

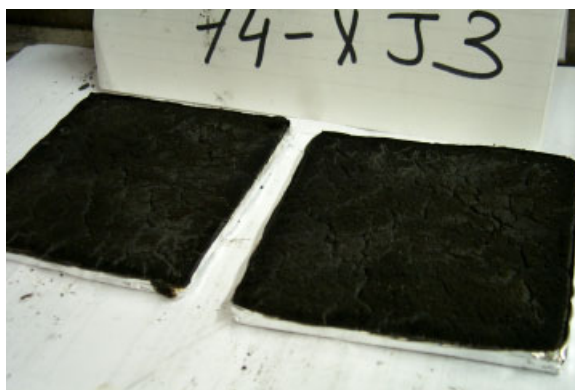


Figure 9. [Right] PS + 16.2 wt% O-MMT sample after burning.

Table IV. Cone calorimeter results for PS + phosphonium fluorinated synthetic mica (P-FSM) samples.

Product	Unit	PS+SMA control	PS+8.3 wt% P-FSM	PS+SWA+8.3 wt% P-FSM	PS control
T_{ig}	s	64	64	65	65
Peak q	kW/m ²	1280.4	586.2	557.3	1293.6
Mean q	kW/m ²	718.8	424.4	370.0	692.4
180sec q	m ² /kg	628.7	514.5	446.1	614.1
300sec q	kW/m ²	377.2	332.5	332.5	368.4
Total q	MJ/m ²	113.1	99.7	99.7	110.5
Effective H	MJ/kg	-30.8	26.6	26.5	30.6

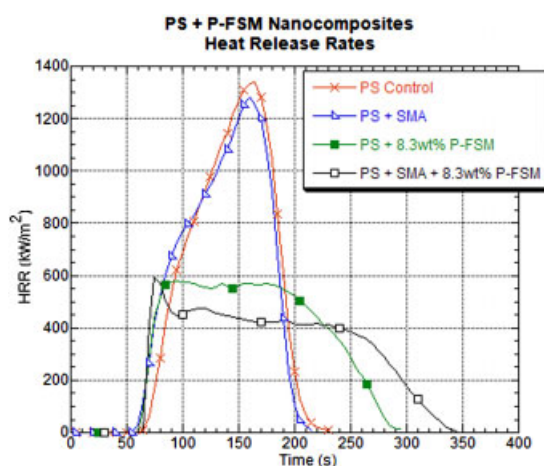


Figure 10. Heat release rate (HRR) curves for PS + Phosphonium FSM (P-FSM) samples.

phosphonium treatment on the P-FSM (triphenyl, *n*-hexadecyl phosphonium) to be thermally stable up to 220°C, as well as having a higher peak decomposition temperature, the lack of T_{ig} reduction suggests that improving the thermal stability of the organic treatment will prevent T_{ig} reduction. Further, improved thermal stability may even prolong T_{ig} . The MLR data collected on the P-FSM samples show again a match between MLR and HRR (Figures 11 and 10, respectively). However, the HRR data in Figure 10 show that the PS + SMA + P-FSM sample has a much lower HRR curve after the initial ignition, suggesting better burn behavior when compared with the sample without SMA. The char formed by the two P-FSM samples (Figures 12 and 13) shows that the P-FSM materials hold onto carbon char during burning, as was seen with the O-FSM samples. Therefore, changing the organic treatment does not seem to change the mechanism by which carbon is trapped in the char of the FSM samples.

3.2. TEM analysis of PS nanocomposites

The TEM analysis was undertaken on most of the samples listed in this study; the PS and PS+SMA control samples were excluded. The TEM analysis showed that the sodium clays

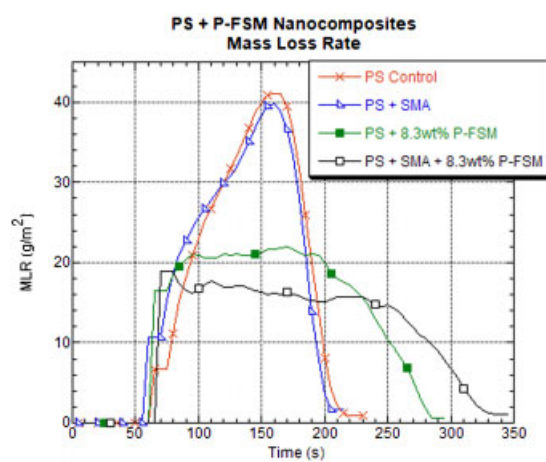


Figure 11. Mass loss rate (MLR) curves for PS + Phosphonium FSM (P-FSM) samples.



Figure 12. [Left] PS + 8.3 wt% P-FSM sample after burning.

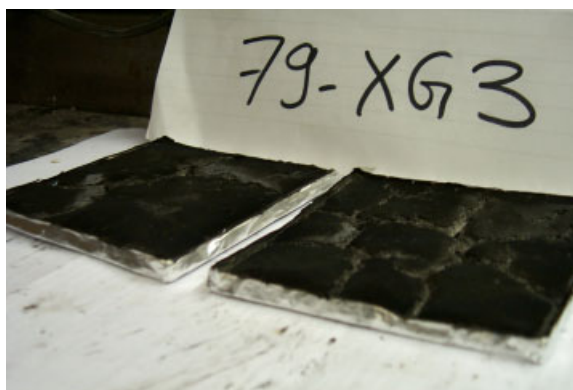


Figure 13. [Right] PS + SMA + 8.3 wt% P-FSM sample after burning.

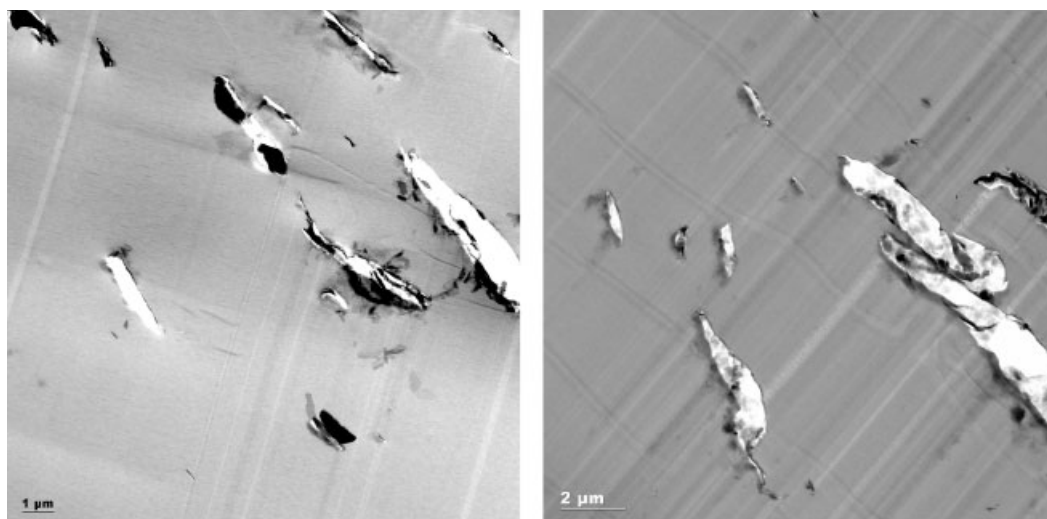


Figure 14. Typical microscale dispersion for sodium clay microcomposite (shown is TEM for PS + 5 wt% NaFSM [Left], PS + 5 wt% NaMMT [Right]).

(NaFSM, NaMMT) only produced microcomposites, with no good dispersion at microscale or nanoscale. In Figure 14 below, the dark spots near the white 'holes' are the NaMMT or NaFSM particles. The holes are created when the clay particle is pulled out of the PS matrix by the TEM sample preparation process. More specifically, the diamond microtome knife very often pulls the microcomposite particles out of the PS matrix, giving a section that appears torn.

The TEM result in Figure 14 is supported by the XRD data showing no change in d-spacing (Table V), indicating that these clays only gave microcomposites. The TEM analysis on the nanocomposites obtained from the organoclays (O-FSM, O-MMT and P-FSM) showed that clay dispersion was good at the microscale and nanoscale (Figure 15). The clay particles are the dark 'wavy' lines in the sample pictures. Interestingly, samples that have organoclays and appear to be actual nanocomposites rarely have the problem observed with the microcomposite samples (Figure 14) when microtomed. The clay particles in nanocomposite samples are not ripped out by the diamond knife, which gives an image (Figure 15) that sticks out from the microcomposite images (Figure 14).

3.3. XRD, TGA analysis of PS nanocomposites

The XRD data (Table V) were collected on all of the PS nanocomposites in this study. As expected, the microcomposites generated from the sodium clays (NaFSM, NaFSM) showed no change in d-spacing. With the exception of the phosphonium clays (P-FSM), all the clays had the same organic treatment, which was dimethyl, bis(hydrogenated tallow) ammonium. Therefore, assuming that the organic treatment will always react the same with the polymer matrix, the clay substrate should have more of an effect on dispersion and d-spacing change than the organic treatment. Again, this assumption only holds if the clays compared all have the same organic treatment which they do in this set. The XRD data (Table V) for the organoclays (O-FSM, O-MMT) are quite interesting. All the O-FSM samples show d-spacing decreases of

Table V. TGA, XRD data for PS nanocomposites.

[wt% inorganic] Sample	TGA Data			XRD Data (nm)	
	dTGA peak (C)	wt% lost @ 700° C	Onset of decomp. (C)	D(100) spacing	d-spacing change
PS + 1 wt% NaFSM	434	99.1	280	1.21	0.01
PS + 5 wt% NaFSM	440	95.4	280	1.22	0.02
PS + 10 wt% NaFSM	437	90.4	280	1.21	0.01
PS + 1.9 wt% [1]O-FSM	441	99	270	3.3	-0.15
PS + 9.3 wt% [5]O-FSM	446	94.5	260	3.19	-0.26
PS + 18.6 wt% [10]O-FSM	443	87.8	225	3.25	-0.2
PS + 1 wt% NaMMT	442	99.1	280	No peak	No peak
PS + 5 wt% NaMMT	441	95.6	280	1.17	0
PS + 10 wt% NaMMT	440	91.7	280	1.19	0.02
PS + 1.6 wt% [1]O-MMT	455	98.8	280	3.23	0.03
PS + 8.1 wt% [5]O-MMT	459	94.9	270	3.23	0.03
PS + 16.2 wt% [10]O-MMT	460	90.5	225	3.25	0.05
PS + 8.3 wt% [5]P-FSM	442	95.6	280	3.69	0.56
PS + SMA + 8.3 wt% [5]P-FSM	451	95.3	280	3.75	0.62
PS + SWA (90/10) control	439	99.9	290	—	—
PS control	438	100	300	—	—

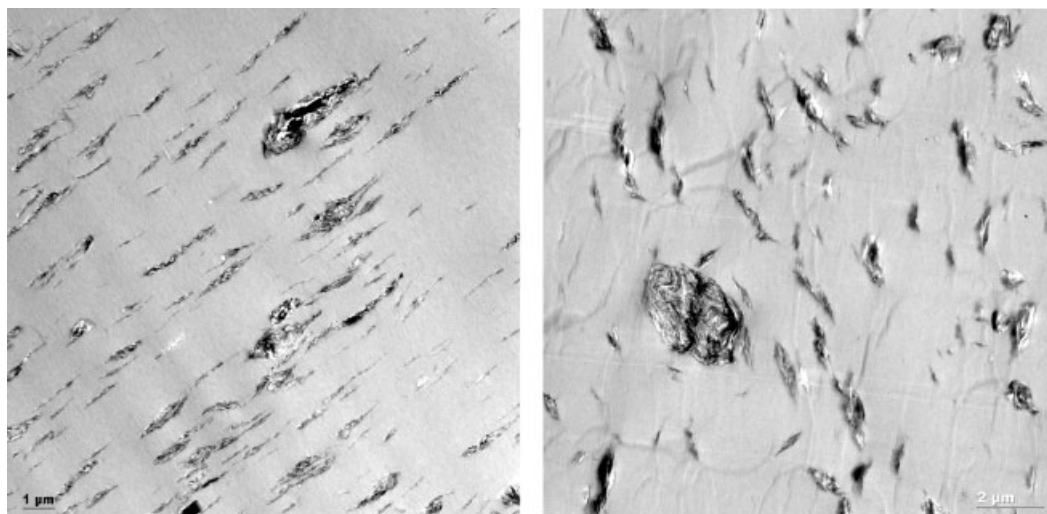


Figure 15. Typical microscale dispersion for organoclay nanocomposite (shown is TEM for PS + 9.3 wt% O-FSM [Left], PS + 8.1 wt% O-MMT [Right]).

0.15 to 0.26 nm, suggesting either organic treatment degradation, or the de-intercalation of excess organic treatment [19]. The latter is more likely as the melt-compounding of these nanocomposites was kept below 200°C. All the O-MMT samples show negligible d-spacing increases, which fall into the region of error, and therefore suggest that no polymer intercalation

or excess organic treatment de-intercalation occurred. Results for the P-FSM samples show d-spacing increases of 0.56 nm in PS, and 0.62 nm in PS+SMA, suggesting polymer intercalation. When the XRD data are combined with the TEM data above, what may be forming is a nanocomposite, but instead of intercalation between single layers of clay, instead polymer surrounds a multi-layer stack, making a stack several clay plates thick, the nanoparticle in the nanocomposite. By traditional definitions of nanocomposites [1], the alkyl ammonium nanocomposites would be reclassified as microcomposites, but given the improvement in flammability performance and the TEM data, these materials are nanocomposites, just not ideal intercalated/exfoliated nanocomposites. More work is needed in the nanocomposite community to better define nanocomposite structure with regard to XRD data.

The TGA data also show some interesting trends with regard to the onset of decomposition temperature. As the loading of organoclay increased, the temperature at which decomposition began decreased. Since the organic treatment on the clay is thermally unstable above 200°C, this suggests that the early decomposition observed by TGA is the organic treatment decomposing before the base polymer. Therefore, as the amount of organoclay is increased in the nanocomposite, more organic treatment will decompose, pushing the onset of decomposition to lower temperatures. Also, as the onset of decomposition moves to lower temperatures, the T_{ig} should decrease as well. With the exception of the microcomposite samples, the TGA data suggest that if an early decomposition is seen by TGA for a nanocomposite, the same nanocomposite will also show a decreased T_{ig} . Therefore, TGA may be a useful screening technique for nanocomposites with differing organic treatments when looking at possible differences in T_{ig} .

4. CONCLUSIONS

With regard to flammability performance, O-MMT and O-FSM nanocomposites behaved similarly within the cone calorimeter, with the O-FSM nanocomposites showing slightly lower HRR values. The NaMMT and NaFSM nanocomposites also behaved similarly, showing only a small reduction in HRR. Therefore, with regard to flammability performance, the natural and synthetic clays were about the same, suggesting that the chemical and physical properties of these two clays do not greatly affect polymer flammability. There were some slight differences between the O-MMT and O-FSM samples with regard to T_{ig} , with the O-MMT samples showing less of a reduction. The use of a thermally stable organic treatment, however, gives a T_{ig} equal to that of PS, suggesting that the organic treatment type has more effect on some flammability measurements (T_{ig}) than the clay type.

The curve shape for the HRR data on all of the PS nanocomposites gives some insight into these materials as potential fire safe materials. UL-94 'V' testing on all of the samples generated in this report gave the same result, regardless of clay loading. The result was a 'not-ratable' or failing rating for the material. The observation during the UL-94 'V' test was that all of the nanocomposites, once exposed to the flame, always ignited, but burned very slowly. This fits with the cone calorimeter HRR curves [22]. When compared with the PS control sample, the PS nanocomposites have a greatly reduced peak and average HRR. Once ignited, all the PS nanocomposites rapidly rise to their reduced peak HRR, and slowly slope down to lower and lower HRR values, whereupon the sample finally extinguishes. The UL-94 test result fits this observation. As for using organoclay alone as a flame retardant to obtain an UL-94 'V' result,

increasing the total loading of organoclay is a possibility, but as clay loading is increased, the nanocomposite benefits are lost. Mechanical properties begin to suffer, and at high loadings, microcomposites of intercalated clay, rather than nanocomposites, are often formed [20,21]. Therefore, it becomes impractical to use nanocomposites alone to impart ignition resistance to polymeric materials. Flame retardancy is achieved with nanocomposites alone, but not enough for an ignition resistance test such as UL-94. The approach to use with nanocomposites is to combine the nanocomposite with another flame retardant, such that the nanocomposite provides the base reduction in flammability, and the secondary flame retardant provides the ignition resistance [4,5,23].

The advantages of synthetic vs natural clays with regard to the polymer flammability of a nanocomposite are not clear when looking just at flammability properties. Since an additional flame retardant will be needed to give a polymer nanocomposite ignition resistance, additional work is needed to determine if a natural or synthetic clay works the same with all flame retardants, or if in the presence of other additives it works differently. Therefore, the results in this paper do not show a clear advantage of a synthetic over a natural clay with regard to polymer flammability, but there are still reasons to choose one type of clay over another for application needs. Synthetic clays have an advantage in color and purity when compared with natural clays, and these can be factors that determine the success of a commercial product. Until more research is done on organoclay nanocomposites with additional flame retardants, the only major differences between a natural and synthetic clay are cost, color and batch-to-batch consistency. The flammability performance of natural- and synthetic clay-nanocomposites is for all practical purposes, the same.

ACKNOWLEDGEMENTS

The authors would like to thank the following people for their assistance: Sylvie Boukami for cone calorimeter testing, Mike Paquette for organoclay synthesis and technical discussions, Andrew Banks for polymer compounding and molding work, and Juan Garces for layered silicate chemistry discussions.

REFERENCES

1. Ray SS, Okamoto M. Polymer/layered silicate nanocomposites: a review from preparation to processing. *Progress in Polymer Science* 2003; **28**:1539–1641.
2. Gilman JW, Jackson CL, Morgan AB, Harris RH, Manias E, Giannelis EP, Wuthenow M, Hilton D, Phillips S. Flammability properties of polymer-layered silicate nanocomposites. Polypropylene and polystyrene nanocomposites. *Chemistry of Materials* 2000; **12**:1866.
3. Gilman JW. Flammability and thermal stability studies of polymer layered-silicate (clay) nanocomposites. *Applied Clay Science* 1999; **15**:31.
4. Zanetti M, Camino G, Canavese D, Moran AB, Lamelas FJ, Wilkie CA. Fire retardant halogen-antimony-clay synergism in polypropylene layered silicate nanocomposites. *Chemistry of Materials* 2002; **14**:189–193.
5. Beyer G. Flame retardant properties of EVA-nanocomposites and improvements by combination of nanofillers with aluminum trihydrate. *Fire and Materials* 2001; **25**:193–197.
6. Dabrowski F, Le Bras M, Cartier L, Bourbigot S. The use of clay in an EVA-based intumescent formulation. Comparison with the intumescent formulation using polyamide-6 clay nanocomposite as carbonisation agent. *Journal of Fire Sciences* 2001; **19**:219–241.
7. Gilman JW, Kashiwagi T. Polymer-layered silicate nanocomposites with conventional flame retardants. In *Polymer-Clay Nanocomposites*, Pinnavaia TJ, Beall GW (eds). Wiley: New York, 2000; 193–206.
8. Weaver CE, Pollard LD (eds). Chapter 5. Smectite. *The Chemistry of Clay Minerals*. Elsevier Scientific Publishing Company: New York, 1973; 55–77.

9. Zhu J, Uhl FM, Morgan AB, Wilkie CA. Studies on the mechanism by which the formation of nanocomposites enhances thermal stability. *Chemistry of Materials* 2001; **13**:4649–4654.
10. Xie W, Gao Z, Pan W-P, Hunter D, Singh A, Vaia R. Thermal degradation chemistry of alkyl quaternary ammonium montmorillonite. *Chemistry of Materials* 2001; **13**:2979.
11. Pauly TR, Pinnavaia TJ. Pore size modification of mesoporous HMS molecular sieve silicas with wormhole framework structures. *Chemistry of Materials* 2001; **13**:987.
12. Kruk M, Jaroniec M, Sayari A. A unified interpretation of high-temperature pore size expansion processed in MCM-41 mesoporous silicas. *Journal of Physical Chemistry B* 1999; **103**:4590.
13. Weiss A. Replication and evolution in inorganic systems. *Angewandte Chemie (International Edition)* 1981; **20**:850 (in English).
14. Zanetti M, Camino G, Thomann R, Mulhaupt R. Synthesis and thermal behaviour of layered silicate-EVA nanocomposites. *Polymer* 2001; **42**:4501–4507.
15. Zanetti M, Camino G, Mulhaupt R. Combustion behaviour of EVA/fluorohectorite nanocomposites. *Polymer Degradation and Stability* 2001; **74**:413–417.
16. Gilman JW, Kashiwagi T, Morgan AB, Harris RH, Brassell LD, VanLandingham M, Jackson CL. Flammability of polymer clay nanocomposites consortium: year one annual report. *National Institute of Standards and Technology Internal Report (NISTIR) 6531*, July 2000.
17. Gilman JW, Kashiwagi T, Nyden M, Brown JET, Jackson CL, Lomakin S, Giannelis EP, Manias E. Flammability studies of polymer layered silicate nanocomposites: polyolefin, epoxy, and vinyl ester resins. *Chemistry and Technology of Polymer Additives*. The Royal Society of Chemistry: Cambridge, 1999; 249–265.
18. Morgan AB, Gilman JW, Jackson CL. Characterization of the dispersion of clay in a polyetherimide nanocomposite. *Macromolecules* 2001; **34**:2735–2738.
19. Morgan AB, Harris JD. Effects of organoclay Soxhlet extraction on mechanical properties, flammability properties and organoclay dispersion of polypropylene nanocomposites. *Polymer* 2003; **44**:2313–2320.
20. Zhulina E, Singh C, Balazs AC. Attraction between surfaces in a polymer melt containing telechelic chains: guidelines for controlling the surface separation in intercalated polymer-clay composites. *Langmuir* 1999; **15**:3935.
21. Ginzburg VV, Singh C, Balazs AC. Theoretical phase diagrams of polymer/clay nanocomposites: the role of grafted organic modifiers. *Macromolecules* 2000; **33**:1089.
22. Bartholmai M, Schartel B. Layered silicate polymer nanocomposites: new approach or illusion for fire retardancy? Investigations of the potentials and the tasks using a model system. *Polymers for Advanced Technologies* 2004; **15**:355–364.